

Coordination Modes of Water-Derived Bridging Ligands in Diiron(III) Complexes: Stabilization of an Oxo-Hydroxo Bridge by Hydrogen Bonding

Miroslav Rapta and Peter Kamaras

Department of Chemistry, Georgetown University
Washington, D.C. 20057

Gregory A. Brewer

Department of Chemistry
The Catholic University of America
Washington, D.C. 20064

Geoffrey B. Jameson*

Department of Chemistry and Biochemistry
Massey University, Palmerston North, New Zealand

Received December 13, 1994

Metalloproteins such as hemerythrin (Hr), ribonucleotide reductase (RR), methane monooxygenase (MMO), and purple acid phosphatases (PAP), including uteroferrin (UF), feature dinuclear iron species multiply bridged by carboxylate residues and, in stable or resting states of the protein, by a single water-derived ligand, such as hydroxo or oxo.¹ However, at intermediate stages of the enzymatic cycle or during (re)formation of the active site, the form and number of water-derived ligands may vary depending on the protein. The coordination spheres of the two iron centers differ due to unsymmetric coordination of histidine (Hr), glutamic acid (MO, RR, PAP), and tyrosine (PAP) residues. Such asymmetry plays important roles in providing selective substrate binding (e.g., a nonbridging peroxy species in oxyHr² and possibly MMO;¹ control of oxidation states (e.g., PAP),³ and stereochemical control of intermediates in the catalytic cycle (e.g., PAP and MMO).^{3,4} Currently there is intense interest in dinuclear iron model systems that have polyfunctional (N_xO_y) ligation,⁵ different coordination of the two iron centers,⁶ and unusual bridging modes of water-derived ligands^{7a-d,h,k,l} and in species which mimic protein-substrate/inhibitor intermediates (e.g., PAP-tetrahedral oxoanion complex⁸).

We have recently developed a synthetic procedure for the preparation of polybenzimidazole ligands, N3O(H)N2-R, that have tridentate and bidentate pendant arms connected by a phenol spacer.⁹ The symmetric analogue proved to be useful for the synthesis of dinuclear phenoxo-bridged complexes which mimic several properties of non-heme oxo-diiron metalloenzymes.¹⁰ The methoxybenzyl species (Scheme 1) binds in a 1:1 manner to iron(III), leading to an unusual diiron(III) species **1** (Figure 1) that not only features terminally coordinated

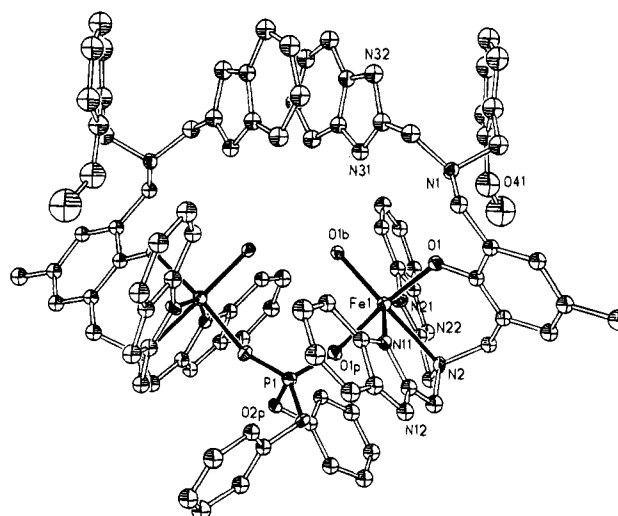
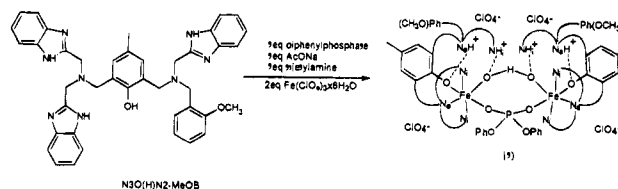


Figure 1. Perspective view of the cation $[\text{Fe}^{\text{III}}(\text{N}_3\text{O}(\text{H})\text{N}_2\text{MeOB})_2(\text{O}\cdots\text{H}\cdots\text{O})(\text{O}_2\text{P}(\text{OPh})_2)\text{Fe}^{\text{III}}]^{4+}$. Hydrogen atoms are omitted, and only labels for non-carbon atoms are shown for clarity. Selected bond lengths (Å) and angles (deg): Fe \cdots Fe' 5.164(2), Fe–O(1) 1.907(10), Fe–O(1b) 1.918(9), Fe–O(1P) 2.030(10), Fe–N(Im) 2.112(13) and 2.117(13), Fe–N(amine) 2.327(12), P–O(1P) 1.488(10), P–O(Ph) 1.587(10), O(1)–C 1.37(2), O(1)–Fe–O(1P) 173.7(4), O(1b)–Fe–O(1) 92.6(4), O(1)–Fe–N(Im) 90.5(4) and 96.2(5), O(1b)–Fe–N(amine) 176.1(5), O(1b)–Fe–O(1P) 93.3(4), O(1b)–Fe–N(Im) 106.6(5) and 101.9(5), N(Im)–Fe–N(Im) 150.7(5), N(Im)–Fe–N(amine) 77.2(5) and 74.2(5), Fe–O(1P)–P 147.0(7), O(1P)–P–O(1P) 121.9(9), O(1P)–P–O(2P) 108.6(5). Hydrogen-bonding details: O–H 1.29, O \cdots (H) \cdots O 2.58(3), O \cdots H \cdots O 164.0°, O \cdots (H)–N(31) 2.92(2), O(1) \cdots (H)–N(1) 2.72(2).

Scheme 1



phenoxo ligands and a μ -diphenyl-phosphato- O,O' bridge but also is the first example of a dinuclear iron complex with an oxo-hydroxo bridge, Fe–O \cdots H \cdots O–Fe. This OHO³⁻ group, which is stabilized by hydrogen bonding to the >N–H groups of the uncoordinated benzimidazole moieties, is suggestive of possible intermediates in the stepwise deprotonation of coordinated water molecule(s), as the OHO³⁻ group is, at least formally, the penultimate species in the hydrolysis of a bis-(aquo)diiron(III) species to a (μ -oxo)diiron(III) product. Scheme 2 illustrates relationships among water-derived ligands coordinated to diiron species; the actual formation of μ -oxo or bis-(μ -oxo) species may employ mechanisms other than step-by-step deprotonation. The following members have been structurally characterized: bis(aquo)diiron(III),^{7a} (μ -(aquo \cdots hydroxo)diiron(III)),^{7b-d} compound **1**, bis(μ -hydroxo)diiron(III),^{1c,7e,g} (μ -oxo- μ -hydroxo)diiron(III),^{7h} (μ -aquo)diiron(II),⁷ⁱ

(6) Available as supporting information.

(7) Available as supporting information.

(8) Available as supporting information.

(9) (a) Kamaras, P.; Cajulis, M. C.; Rapta, M.; Brewer, G. A.; Jameson, G. B. *J. Am. Chem. Soc.* 1994, 116, 10334–10335. (b) The compound was synthesized analogously to those described in ref 9a. The N2-MeOB branch of the ligand was synthesized by the reductive amination of 2-methoxybenzaldehyde with 2-(aminomethyl)benzimidazole as described: Rapta, M.; Kamaras, P.; Jameson, G. B. In preparation.

(10) (a) Suzuki, M.; Oshio, H.; Uehara, A.; Endo, K.; Yanaga, M.; Kida, S.; Saito, K. *Bull. Chem. Soc. Jpn.* 1988, 61, 3970–3913. (b) Suzuki, M.; Uehara, A.; Endo, K. *Inorg. Chim. Acta* 1986, 123, L9–L10.

(1) (a) Que, L., Jr.; True, A. E. In *Progress in Inorganic Chemistry*; Lippard, S., Ed.; J. Wiley & Sons: New York, 1990; Vol. 38, pp 97–201. (b) Vincent, J. B.; Olivier-Lilley, G. L.; Averill, B. A. *Chem. Rev.* 1990, 90, 1447–1467. (c) Kurtz, D. M., Jr. *Chem. Rev.* 1990, 90, 585–606. (d) Feig, A. L.; Lippard, S. J. *Chem. Rev.* 1994, 94, 759–805.

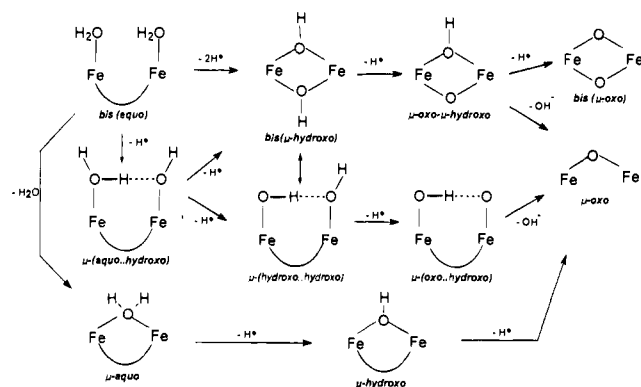
(2) Holmes, M. A.; Le Trong, I.; Turley, L. C.; Stenkamp, R. E. *J. Mol. Biol.* 1991, 218, 583–593.

(3) Dietrich, M.; Münstermann, D.; Suerbaum, H.; Witzel, H. *Eur. J. Biochem.* 1991, 199, 105–113.

(4) Liu, K. E.; Johnson, C. C.; Newcomb, M.; Lippard, S. J. *J. Am. Chem. Soc.* 1993, 115, 939–947.

(5) (a) Krebs, B.; Schepers, K.; Bremer, B.; Henkel, G.; Althaus, E.; Müller-Warmuth, Griesar, K.; Haase, W. *Inorg. Chem.* 1994, 33, 1907–1914. (b) Campbell, V. D.; Parson, E. J.; Pennington, W. T. *Inorg. Chem.* 1993, 32, 1773–1778. (c) Neves, A.; de Brito, M. A.; Vencato, I.; Drago, V.; Griesar, K.; Haase, W.; Mascarenhas, Y. P. *Inorg. Chim. Acta* 1993, 214, 5–8. (d) Sandi-Urena, S.; Parsons, E. J. *Inorg. Chem.* 1994, 33, 302–305. (e) Neves, A.; Erthal, S. M. D.; Drago, V.; Griesar, K.; Haase, W. *Inorg. Chim. Acta* 1992, 197, 121–124. (f) Yan, S.; Que, L., Jr.; Taylor, L. F.; Anderson, O. P. *J. Am. Chem. Soc.* 1988, 110(15), 5223–5224. (g) Murch, B. P.; Bradley, F. C.; Boyle, P. D.; Papaefthymiou, V.; Que, L., Jr. *J. Am. Chem. Soc.* 1987, 109, 7993–8003. (h) Mockler, G. M.; de Jersey, J.; Zerner, B.; O'Connor, Ch. J.; Sinn, E. *J. Am. Chem. Soc.* 1983, 105, 1891–1893.

Scheme 2



(μ -hydroxo)diiron(III),^{7j,8e} (μ -oxo)diiron(III),^{1c,7l} and bis(μ -oxo)diiron(III).^{7k} Such species are relevant to the stereochemistry of non-heme iron-oxo proteins, since the exact nature of the aquo-derived bridging ligand(s) and the transformations during the active site formation and enzymolysis remain uncertain for at least some stages for all members of this family of metalloenzymes.

While the crystal structure of **1** lacks high precision,¹¹ the stereochemistry is unequivocal (Scheme 1, Figure 2, supporting information): the Fe–O(oxo/hydroxo) bond length of 1.918(9) Å is shorter than that observed in the μ -(aquo...hydroxo) species (2.040(9) and 1.913(7) Å),^{7b–d} is marginally shorter than that observed for the μ -oxo- μ -hydroxo isomer (O/OH disordered; average Fe–O, 1.94 Å),^{7h} and is intermediate between that found for (μ -oxo)diiron(III) species (1.73 Å^{11a} to 1.84 Å^{10c})^{7h} and (μ -hydroxo)diiron(III) species (1.95–1.98 Å);^{7e–g} the proton between the two oxygen atoms (separated by 2.58(3) Å) is observed in difference Fourier maps and can be refined satisfactorily; the uncoordinated benzimidazole moieties are oriented so as to optimally hydrogen bond to the oxo-hydroxo moiety (N(H)...O 2.92(2) Å); the uncoordinated, protonated amine atoms are oriented to hydrogen bond to the terminal phenoxo species, which itself has an Fe–O separation of 1.907–(10) Å, similar to the separations found for other terminally coordinated phenoxo species.⁵ The short distance between benzimidazole nitrogen N32 and perchlorate oxygen (2.88(3) Å), charge balance, and elemental analysis strongly support double protonation of the ligand. The Fe–O...O angle of the Fe–OHO–Fe moiety of **1** is distinctively obtuse, leading to the long Fe...Fe separation of 5.164(2) Å and an unusually obtuse Fe–O–P angle of 147.0(7)°, in contrast with the μ -(aquo...hydroxo) species where the Fe...Fe separation is 3.389(2) Å,^{7b} and there is a single-atom oxo ligand as the second bridge.

The concentration-independent UV–visible spectrum of **1** in acetonitrile shows two overlapping bands at ~330 ($\epsilon = 3955 \text{ M}^{-1} \text{ cm}^{-1}/\text{Fe}^{\text{III}}$) and ~380 (~2200) nm, and a phenolate-to-Fe(III) charge transfer band at 576 nm (1650) that is responsible for the purplish color of the complex. Very weak antiferromagnetic coupling is observed ($J = -3 \text{ cm}^{-1}$, $\mathbf{H} = -2/S_1 - mS_2$);¹³ strong coupling remains uniquely consistent with a μ -oxo moiety. The ¹H NMR spectrum of **1** exhibits paramagnetically shifted peaks up to 70 ppm downfield, consistent with **1** maintaining its integrity in solution. Cyclic voltammetry of **1** in acetonitrile (Figure 3, supporting information) shows two quasi-reversible waves at –235 mV ($\Delta E_1 = 87 \text{ mV}$) and 165 mV ($\Delta E = 82 \text{ mV}$) vs SCE¹⁴ that exhibit some concentration dependence only for very dilute solutions. Reversible redox processes for both the Fe^{III}₂/Fe^{II}Fe^{III} and the Fe^{III}Fe^{II}/Fe^{II}₂ couples are rare, except for species held together by a bridging phenoxo or alkoxo group.¹² For **1**, however, the proximity of protons on the uncoordinated N2 arm may allow the facile transfer of protons onto the OHO³⁻ moiety and quasi-reversible behavior. Similar acid–base-active, noncoordinated residues

may be responsible for the extreme pH sensitivity of redox behavior for Uf.¹⁵ The synthesis of a mixed-valence species using iron(II) salts has been unsuccessful due to rapid two-electron oxidation leading to the Fe^{III}₂ species characterized. While **1** does not correspond to any of the forms of presently characterized dinuclear iron centers, the novel oxo...hydroxo bridge does illumine a general pathway by which the coordination spheres of dinuclear metal complexes can be expanded to accommodate water-derived species produced or taken up in the course of enzymolysis. It also features two geometrical motifs relevant to this group of metalloenzymes: the structure of **1** is the first example of a monophosphato bridged species with a terminal phenolato coordination (cf. PAPs), and **1** has an uncoordinated tyrosine-like (methoxyphenyl) group in close proximity (Fe...O41 4.55(3) Å) to the diiron core as found in RR and recently modeled with a tethered phenoxyl radical.¹⁶

Acknowledgment. We thank the National Science Foundation for Grant CHE-9125394 in support of the purchase of the diffractometer. We also thank the Department of Chemistry, Georgetown University, for partial financial support of this research.

Supporting Information Available: References 6–8 and Figures 2 and 3 as well as complete tables of crystal data and structure refinement, atomic coordinates and derived parameters, stereodiagram of the molecular packing, and details of magnetic susceptometry (16 pages). This material is contained in many libraries on microfiche, immediately follows this article in the microfilm version of the journal, can be ordered from the ACS, and can be downloaded from the Internet; see any current masthead page for ordering information and Internet access instructions.

JA944032W

(11) (a) Dark crystals of [Fe₂(N3O⁻·N2H₂(²⁺·MeOB)₂(O₂P(OC₆H₅)₂)(O...H...O)](ClO₄)₄·6H₂O appeared after several days from a solution of 0.2 g (0.3 mmol) of N3O(H)N2-MeOB, 0.075 g of hydrogen diphenyl phosphate (0.3 mmol), and 42 μ L of triethylamine (0.3 mmol) in 50 mL of absolute alcohol to which was added 0.27 g of Fe(ClO₄)₃·6H₂O (0.6 mmol) in 10 mL of absolute ethanol. Yield: 0.125 g (~19%). IR [KBr, cm⁻¹]: 1590 (δ_{DPP}), 1490 (δ_{L}), 1476 (δ_{DPP}), 1455 (δ_{L}), 1253 ($\nu_{\text{PNC-OCH}_3}$), 1220 ($\nu_{\text{PNC-O}}$), 1101 (ClO₄⁻), 938 (δ_{DPP}), 751 (δ_{L}), 691.5 (δ_{DPP}), 625 (ClO₄⁻) and 540 (δ_{DPP}). Anal. Calcd for C₉₄H₉₃N₁₆O₁₀P₁Fe₂·4ClO₄·6H₂O: C, 50.77; H, 4.73; N, 10.08; P, 1.39; Fe, 5.03; Cl, 6.39. Found: C, 50.84; H, 4.53; N, 9.73; P, 1.28; Fe, 4.54 (5.01 by atomic absorption spectroscopy with standards containing similar matrix elements); Cl, 6.15. The same product (identical spectral and unit cell parameters) was obtained in 65% yield by the following procedure: to a solution of 0.2 g (0.3 mmol) of N3O(H)N2-MeOB and 0.037 g of hydrogen diphenyl phosphate (0.15 mmol) in 50 mL of absolute alcohol was added 0.137 g of Fe(ClO₄)₃·6H₂O (0.3 mmol) and 42 μ L of triethylamine (0.3 mmol). After 1 h the solid inorganic salts were removed by filtration and the complex was precipitated with diethyl ether and recrystallized from methanol–acetone solution. (b) Crystal data for C₉₄H₉₃N₁₆O₁₀P₁Fe₂·4ClO₄·6H₂O (**1**) at –70 °C, $M_r \sim 2.243$: $C2/c$, $a = 22.662(6) \text{ \AA}$, $b = 16.187(5) \text{ \AA}$, $c = 28.937(6) \text{ \AA}$, $\beta = 105.84(7)^\circ$, $V = 10212(4) \text{ \AA}^3$, $D_{\text{calcd}} = 1.459 \text{ g cm}^{-3}$, $\mu(\text{Mo K}\alpha) = 0.58 \text{ mm}^{-1}$. A total of 6536 reflections (5430 unique, $R_{\text{merge}}(F^2) = 0.073$) was collected on a Siemens P4/RA diffractometer at 203 K with graphite-monochromated Mo K α radiation ($1.6^\circ < \theta < 22.3^\circ$). The structure was solved by direct methods (SHELXS-90) and refined on F^2 by means of SHELXL-93. The discrepancy index (on F^2) is 0.287 (conventional R for those data where $I > 2\sigma(I)$ is 0.081); $\Delta\rho(\text{max/min}) = 0.364/-0.277 \text{ e}\cdot\text{\AA}^{-3}$. Hydrogen atoms on the bridging oxo-hydroxo moiety and a tertiary nitrogen of the uncoordinated pendant arm were found and refined isotropically. All other hydrogen atoms are constrained to ride on their attached carbon atoms with appropriate geometry. The current R (on F^2) is rather high, due to small crystal size, substantial motion of parts of the uncoordinated arm, and open crystal packing leading to disordered solvate and perchlorate species.

(12) (a) Jang, H. G.; Hendrich, M. P.; Que, L., Jr. *Inorg. Chem.* **1993**, *32*, 911–918. (b) Turnowski, P. N.; Armstrong, W. H.; Roth, M. E.; Lippard, S. J. *J. Am. Chem. Soc.* **1990**, *112*, 681–690. (c) Armstrong, W. H.; Lippard, S. J. *J. Am. Chem. Soc.* **1985**, *107*, 3730–3731.

(13) Magnetic susceptibility data were measured and evaluated as described elsewhere^{6f} and are available as supporting information.

(14) Cyclic voltammetry measurements were carried out in acetonitrile at several concentrations (0.02, 0.05, 0.20, and 0.50 mM) and a sweep rate of 100 mV/s; with glassy carbon working electrode, platinum reference and counter electrodes, and 0.1 M tetra-*n*-butylammonium hexafluorophosphate as a supporting electrolyte. Potentials were corrected to the SCE standard electrode by measuring the ferrocenium/ferrocene couple under the same conditions.

(15) Wang, D. L.; Holz, R. C.; David, S. S.; Que, L., Jr.; Stankovitch, M. T. *Biochemistry* **1991**, *30*, 8187–8194.

(16) Goldberg, D. P.; Kouloughiotis, D.; Brudvig, G. W.; Lippard, S. J. *J. Am. Chem. Soc.* **1995**, *117*, 3134–3144.